Tetrahedron Vol. 49, No. 5, pp. 1079-1090, 1993
Printed in Great Britain

0040-4020/93 $6.00+.00

Mechanistic Studies on the Asymmetric Addition of HCN to Aldehydes Catalysed by Cyclo[(S)-His-(S)-Phe]

David J. P. Hogg and Michael North*

Department of Chemistry, University of Wales, Bangor, Gwynedd, LL57 2UW

(*Received in UK* 8 *October* 1992)

Key Words Cyclo[(S)-Phenylalanyl-(S)-Histidyl]; Conformation; Hydrocyanation; Asymmetric; Mechanism

Abstract: *The nature of the interaction between HCN and cyclo[(S)-His-(S)-Phe] during the asymmetric hydrocyanation of benzaldehyde is investigated by variable pH nmr spectroscopy. The structure of the protonated form of cyclo[(S)-His-(S)-Phe] is determined by variable temperature NMR and molecular mechanics calculations*

Cyanohydrins are versatile synthetic intermediates[1], which are readily prepared from aldehydes and cyanide[2]. However, cyanohydrins prepared in this way, are obtained as a racemate unless chirality is already present in the aldehyde. Recently, there has been much interest in the use of chiral catalysts to promote this reaction, giving cyanohydrins with high enantiomeric excesses[3-5]. Amongst the various catalysts proposed for this reaction[2], the most widely used and versatile is the diketopiperazine (1) derived from (S)-phenylalanine and (S)-histidine originally introduced by Inoue *et al*, which catalyses the addition of HCN to aromatic aldehydes giving cyanohydrins with an enantiomeric excess greater than 80%[4], and with aliphatic aldehydes giving enantiomeric excesses greater than 30%[5].

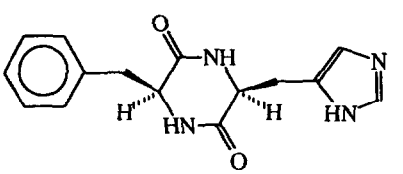

(1)

Until very recently, no mechanistic information on this catalytic, asymmetric, carbon-carbon bond forming reaction was available. We undertook a conformational study of compound (1) using nmr and molecular mechanics techniques[6], and showed that in solution the catalyst exists as a mixture of two conformations as shown in Figure 1. The structure of the major conformer of dipeptide (1) was also investigated by de-Vries *et al.* using nmr and semiempirical molecular orbital calculations[7]. In the same paper, the interaction of HCN with 4-methyl imidazole was investigated using semiempirical MO calculations, and the results used to propose a structure for the transition state of the reaction between HCN and benzaldehyde catalysed by (1). In this paper, we present the results of a study of the effect of acids, including HCN on the conformation of catalyst (1) using nmr techniques. The results are used to investigate the nature of the interaction between catalyst (1) and HCN.

Figure 1: The Structure of a) the Major, and b) the Minor Conformer of Compound (1) Present in Solution.

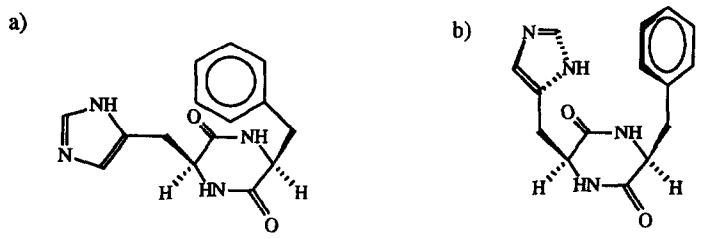

Variable pH NMR Studies

It seemed likely that during a catalytic reaction involving HCN and compound (1), the HCN would associate with the imidazole ring. A comparison of the pKa values of the imidazolium cation (6.95) and HCN (9.22), suggested that this would be a covalent, hydrogen bonded interaction rather than an ionic one. However, as in compound (1) the imidazole hydrogen is involved in an intramolecular hydrogen bond[6] which could affect the pKa of the imidazole ring, it was felt prudent to check this. To do this, the ^1H nmr spectrum of compound (1) dissolved in DMSO-d_6 was recorded under neutral and strongly acidic conditions (by the addition of trifluoroacetic acid). The unprotonated spectrum is shown in Figure 2a, and the corresponding protonated spectrum in Figure 2b. The spectrum shown in Figure 2a has already been interpreted in detail[6], and this will not be repeated here, suffice to say that evidence of a major and a minor conformation can be seen, and that the unusually high field chemical shift observed for one of the histidine-β-protons (1.6ppm) indicates that the major conformer has the structure shown in Figure 1a. The minor conformer has the structure shown in Figure 1b as determined by its coupling constants[6].

The protonated spectrum shown in Figure 2b shows a number of changes compared to the unprotonated spectrum. The first of these is that only one set of peaks is observed in the protonated spectrum, indicating that only one conformation is now present in solution. A ^1H-^1H COSY spectrum allowed all of the peaks in this spectrum to be assigned, and the effect upon chemical shifts and coupling constants of protonating the imidazole ring could then be determined. Both NH resonances shift downfield, in the case of the Phe-NH this is from 8.1 to 8.3ppm, and for His-NH from 7.75 to 8.0ppm. Both imidazole CH protons also shift downfield, H2 from 7.5 to 8.9ppm, and H5 from 6.55 to 6.9ppm. These values are however very similar to those observed for the unprotonated form of compound (1) in CD_3OD (8.74 and 6.95ppm respectively). The shift of the resonances of the imidazole protons of compound (1) on changing the solvent has been interpreted in terms of a change from a hydrogen bonded to a non hydrogen bonded conformer. The two α-CH resonances are only slightly shifted, Phe-α-CH from 4.1 to 4.2ppm, and His-α-CH from 3.8 to 3.95ppm. The most dramatic change in the spectrum concerns the Phe-β-CH_2 resonance, which in the unprotonated spectrum occurs as a multiplet at 2.8ppm. In the protonated spectrum however, this splits into two well resolved resonances (3.1ppm, dd *J* 13.5 and 3.7Hz; 2.85ppm, *J* 13.5 and 5.0Hz). The His-β-CH_2 resonances undergo no change in chemical shift, and only minor changes in coupling constants on protonation (2.48ppm, dd *J* 14.8 and 4.5Hz; 1.65ppm, dd *J* 14.8 and 8.4Hz for the protonated compound as opposed to 2.51ppm, dd *J* 14.5 and 3.5Hz; 1.55ppm, dd *J*14.5 and 8.7Hz for the unprotonated form).

The nmr spectrum of the TFA salt of compound (1) was also recorded in CD_3OD. Compared to the unprotonated form of dipeptide (1), the salt is much more soluble in this solvent. The spectrum in CD_3OD is

comparable to that in DMSO-d_6, in that only one set of peaks are observed, and the $PhCH_2$ resonances are resolved into two double doublets.

A comparison of the unprotonated and protonated spectra indicates that the protonated structure has the same conformation as the major conformer present in the unprotonated structure as shown in Figure 1a. In particular, one of the His-β-CH_2 protons occurs at 1.6ppm in both spectra, indicating that it is being shielded by the phenyl ring. Furthermore, the coupling constants for the histidine resonances are almost identical for the protonated and unprotonated structures indicating that no major conformational change has occured in that half of the molecule.

Figure 2: Proton NMR Spectra of Compound (1) Dissolved in DMSO-d_6.

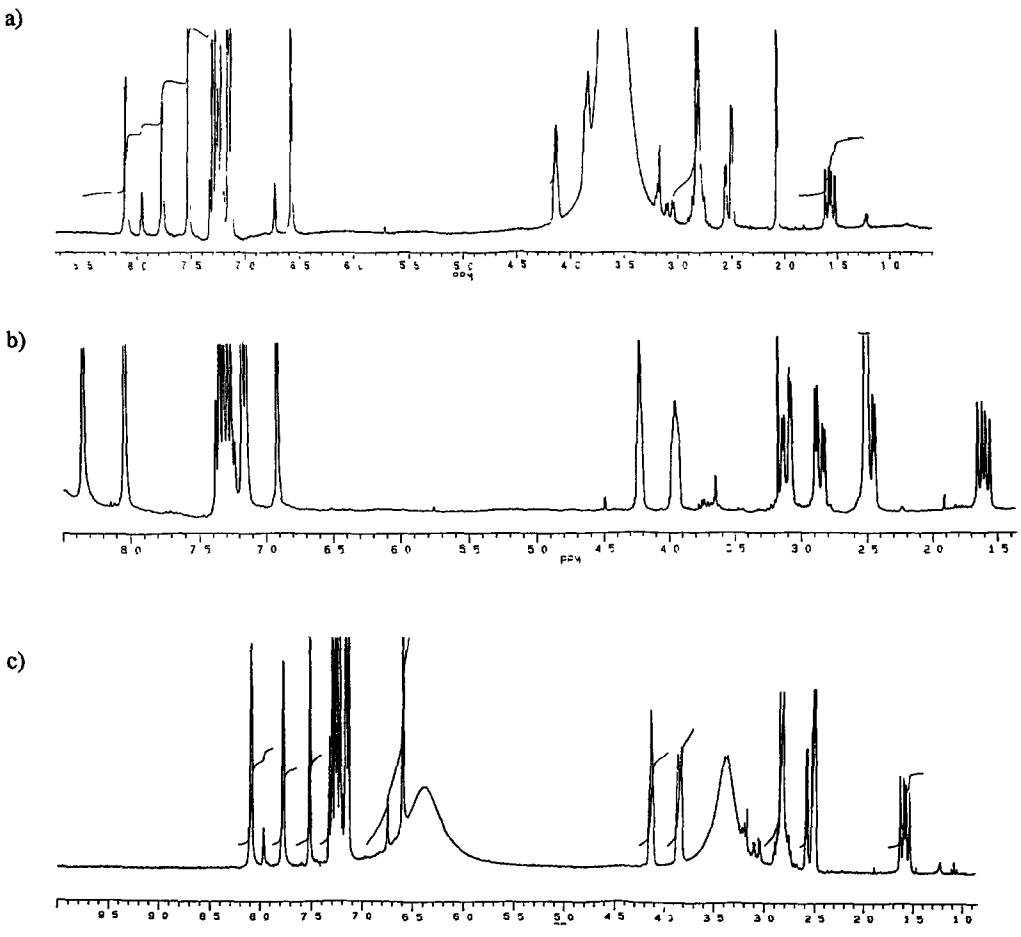

a) Normal spectrum of compound (1); b) Spectrum of compound (1) with TFA added; c) Spectrum of compound (1) with HCN added.

The absence of a second conformation in the protonated structure can be explained by the structure of the minor conformer present in the unprotonated spectrum. This has a structure in which the two aromatic rings face one another across the diketopiperazine ring as shown in Figure 1b, and is thought to be stabilised by π–π interactions between the two aromatic systems[8]. When the imidazole ring is protonated, the electron density in that ring is reduced, which will reduce any π–π interactions with the phenyl ring, and so destabilise this conformation.

Variable Temperature NMR Studies

In order to further investigate how similar the conformations of protonated and unprotonated (1) were, a variable temperature nmr study was carried out. Spectra were recorded at temperatures between -85°C and 60°C in CD_3OD, and between 27°C and 130°C in DMSO-d_6. The results are recorded in Tables 1 and 2. The higher field His-β proton (β2) undergoes a change in chemical shift from 0.6ppm at -85°C, to 2.41ppm at 130°C (1.1×10^{-2} ppm/K in CD_3OD, and 7.4×10^{-3} ppm/K in DMSO). The explanation of this shift is as for the unprotonated compound described previously, namely that the phenyl ring is rotating about the α–β bond.

Table 1: Variable Temperature NMR Results on the TFA Salt of Compound (1) in DMSO.

Temp °C	Imid H2	Imid H5	Phe α-CH	His α-CH	Phe β1	Phe β2	His β1	His β2
130	8.57ppm d 1.3	7.00ppm s	4.21ppm t 4.8	4.10ppm t 5.6	3.05-3.00ppm multiplet		2.73ppm dd 15.0,5.5	2.41ppm dd 15.1,7.0
120	8.61ppm d 1.3	7.00ppm s	4.21ppm br	4.10ppm t 5.4	3.05-2.95ppm multiplet		2.72ppm dd 15.1,5.4	2.40ppm dd 15.1,7.1
110	8.64ppm d 1.2	6.99ppm s	4.20ppm br	4.09ppm t 5.7	3.10-2.90ppm multiplet		2.69ppm dd 15.1,5.3	2.35ppm dd 15.0,7.1
100	8.67ppm d 1.3	6.99ppm s	4.21ppm t 4.8	4.06ppm t 5.9	3.04ppm dd 13.7,4.8	2.95ppm dd 13.7,5.0	2.67ppm dd 15.0,5.3	2.24ppm dd 15.1,7.3
90	8.70ppm d 1.3	6.99ppm s	4.21ppm m	4.05ppm t 6.0	3.05ppm dd 13.8,4.7	2.94ppm dd 13.7,5.0	2.66ppm dd 15.1,5.1	2.20ppm dd 15.1,7.3
80	8.73ppm d 1.4	6.98ppm s	4.21ppm t 4.6	4.04ppm t 5.1	3.06ppm dd 13.8,4.5	2.93ppm dd 13.7,5.0	2.63ppm dd 15.1,5.1	2.14ppm dd 15.1,7.5
70	8.77ppm d 1.3	6.97ppm s	4.21ppm br	4.03ppm br	3.06ppm dd 13.6,4.3	2.92ppm dd 13.6,5.0	2.60ppm dd 15.0,4.9	2.06ppm dd 15.1,7.4
60	8.81ppm d 1.2	6.96ppm s	4.21ppm br	4.01ppm t 6.1	3.07ppm dd 13.6,4.3	2.90ppm dd 13.7,5.1	2.57ppm dd 15.1,4.8	1.98ppm dd 15.0,7.7
50	8.84ppm d 1.2	6.95ppm s	4.21ppm br	4.00ppm br	3.08ppm dd 13.6,4.2	2.89ppm dd 13.6,5.0	2.55ppm part hidden	1.89ppm dd 15.0,8.0
40	8.86ppm s	6.93ppm s	4.21ppm br	3.97ppm br	3.08ppm dd 13.5,4.0	2.87ppm dd 13.5,5.0	2.50ppm part hidden	1.78ppm dd 14.8,8.2
27	8.92ppm s	6.91ppm s	4.19ppm br	3.97ppm br	3.10ppm dd 13.5,3.7	2.85ppm dd 13.5,5.0	2.48ppm dd 14.8,4.5	1.65ppm dd 14.8,8.4

Coupling constants are in Hz, and are reported as they appear in the spectrum, they have not been corrected for second order effects. Hidden means that the peak was coincident with a solvent peak, part hidden means that part of the peak was coincident with a solvent peak so the coupling constants could not be evaluated.

Table 2: Variable Temperature NMR Results on the TFA Salt of Compound (1) in CD_3OD.

Temp °C	Imid H2	Imid H5	Phe α-CH	His α-CH	Phe β1	Phe β2	His β1	His β2
60	8.60ppm d 1.2	6.98ppm s	4.34ppm td 4.6,1.3	4.09ppm ddd 7.1,5.4,1.3	3.17ppm dd 13.9,4.5	2.99ppm dd 13.9,4.7	2.53ppm dd 15.2,5.4	2.13ppm dd 15.2,7.1
50	8.63ppm d 1.3	6.97ppm s	4.35ppm td 4.6,1.3	4.07ppm ddd 8.6,5.3,1.3	3.19ppm dd 13.8,4.3	2.98ppm dd 13.8,4.8	2.51ppm ddd 15.2,5.3,0.8	2.05ppm dd 15.2,7.3
40	8.65ppm d 1.2	6.97ppm s	4.35ppm td 4.5,1.3	4.07ppm dd 7.4,5.2	3.20ppm dd 13.8,4.2	2.98ppm dd 13.8,4.8	2.50ppm dd 15.3,5.2	1.98ppm dd 15.1,7.5
30	8.68ppm d 1.3	6.96ppm s	4.36ppm td 5.0,1.3	4.05ppm ddd 7.7,5.0,1.3	3.22ppm dd 13.7,3.9	2.96ppm dd 13.7,4.8	2.48ppm dd 15.2,5.0	1.88ppm dd 15.2,7.7
20	8.74ppm d 1.4	6.94ppm s	4.37ppm t 3.6	4.01ppm dd 8.3,4.8	3.25ppm dd 13.6,3.7	2.94ppm dd 13.7,4.8	2.45ppm dd 15.1,4.8	1.67ppm dd 15.1,8.3
-10	8.77ppm s	6.93ppm s	4.37ppm t 3.6	4.01ppm dd 8.3,4.5	3.25ppm part hidden	2.94ppm dd 13.7,4.5	2.45ppm dd 15.0,4.6	1.52ppm broad
-20	8.81ppm s	6.93ppm s	4.38ppm t 3.6	3.97ppm dd 9.1,4.3	3.26ppm part hidden	2.93ppm dd 13.7,4.7	2.45ppm dd 14.9,4.3	1.35ppm dd 14.9,9.1
-30	8.83ppm s	6.93ppm s	4.39ppm t 3.6	3.95ppm dd 9.4,4.0	hidden	2.93ppm dd 13.7,4.8	2.45ppm dd 14.8,4.0	1.25ppm dd 14.8,9.7
-40	8.86ppm s	6.95ppm s	4.40ppm br s	3.94ppm dd 9.6,3.8	hidden	2.92ppm dd 13.7,4.7	2.47ppm dd 14.6,3.8	1.07ppm dd14.6,10.9
-50	8.89ppm s	6.96ppm s	4.41ppm br s	3.92ppm dd 10.1,3.4	hidden	2.92ppm dd 13.5,5.0	2.48ppm dd 14.7,3.5	0.97ppm t 12.0
-60	8.91ppm s	6.98ppm s	4.41ppm br s	3.92ppm dd 10.2,3.2	hidden	2.92ppm dd 13.1,4.3	2.50ppm br d 11.3	0.85ppm broad
-70	8.93ppm s	6.99ppm s	4.42ppm br s	3.91ppm dd 10.6,3.1	3.34ppm part hidden	2.93ppm dd 12.8,4.6	2.50ppm br d 11.6	0.78ppm dd14.0,11.3
-80	8.96ppm s	7.01ppm s	4.43ppm br s	3.90ppm dd 10.6,3.0	hidden	2.94ppm br d 10.1	2.52ppm br d 13.1	0.66ppm br t 12.5
-85	8.97ppm s	7.02ppm s	4.44ppm br s	3.90ppm br d 3.6	hidden	2.95ppm br d 10.3	2.53ppm br d 11.9	0.60ppm br t 12.5

Footnotes as for Table 1

At low temperature, the barrier to this rotation becomes more significant, so rotation is suppressed resulting in the phenyl ring spending more time in the global minimum conformation and hence the His-β2 proton becoming more shielded. Conversely, as the temperature is raised, rotation of the phenyl ring becomes easier, so the His-β2 proton becomes less shielded. The His α–β2 coupling constant decreases steadily from 11.3Hz to 7.0Hz as the temperature is raised. Molecular modelling results (*vide infra*) show that this is consistent with the imidazole being stationary at low temperature, but rotating about the α–β bond as the temperature is raised. This is in contrast to the results on the unprotonated compound, where the histidine coupling constants show no temperature effect, suggesting that the imidazole ring does not rotate about the α–β bond[6].

The lower field His-β proton (β1) by comparison, has a chemical shift which varies much less with temperature, between -85°C (2.53ppm), and -30°C (2.45ppm), it varies at a rate of -1.5×10^{-3} ppm/K. Above 20°C however, the direction of change of chemical shift reverses, and the resonance shifts from 2.48ppm at 27°C, to 2.73ppm at 130°C (2.4×10^{-3} ppm/K). This inversion of the direction of change of chemical shift is not due to a change in the solvent at 20°C, as it is also seen in the CD_3OD spectra at temperatures above

20°C. An explanation of this change is given later in this paper (*vide infra*). The His α–β1 coupling constant increases from 3.0 to 5.5Hz as the temperature increases. This is the opposite change to that observed for the α–β2 coupling constant, and is again consistent with a model in which the imidazole ring starts to rotate as the temperature increases (*vide infra*). The spectrum recorded at 50°C in CD_3OD shows an additional 0.8Hz coupling constant which is thought to be an allylic coupling to H5 of the imidazole ring.

The high field Phe-β proton (β2) also undergoes a reversal of direction of change of chemical shift, the chemical shift moves slightly to higher field between -85°C and -60°C (-1.2×10^{-3} ppm/K), but at temperatures above -40°C, this reverses and the chemical shift moves to lower field in both CD_3OD (2.92ppm at -40°C to 2.99ppm at 60°C (7×10^{-4} ppm/K)) and in DMSO (2.85ppm at 27°C to 2.99ppm at 100°C (1.9×10^{-3} ppm/K)), until at 110°C it merges with the other Phe-β proton. An explanation of this behaviour is given later in this paper (*vide infra*). The Phe α–β2 coupling constant shows no significant change over the temperature range.

The lower field Phe-β proton (β1) shows a steady shift to higher field as the temperature increases. In CD_3OD, this is from 3.34ppm at -70°C to 3.17ppm at 60°C, a rate of -1.3×10^{-3} ppm/K, whilst in DMSO the shift is from 3.10ppm at 27°C to 3.04ppm at 100°C, at a rate of -8.2×10^{-4} ppm/k. At temperatures above 100°C, this peak merges with the other Phe-β proton. The Phe α–β1 coupling constant can only be calculated at temperatures above 20°C, and it shows a steady increase from 3.7Hz to 4.8Hz as the temperature increases. This variation in chemical shift and coupling constant is consistent with a model in which rotation about the Phe α–β bond increases as the temperature increases.

The His-α proton resonance shifts steadily to lower field as the temperature increases, from 3.90ppm at -85°C to 4.10ppm at 130°C (1.3×10^{-3} ppm/K in both CD_3OD and DMSO). These results are again consistent with the phenyl group rotating about the α–β bond, and shielding the His-α resonance more at low temperature. The effect of changing the temperature on the His α–β1 and His α–β2 coupling constants has already been discussed, however at 30°C and above in CD_3OD, an additional coupling constant of 1.3Hz is observed. This is a cross ring ^5J coupling to the Phe-α proton, and indicates that the diketopiperazine ring is flat[9].

The Phe-α resonance undergoes a very small shift to higher field as the temperature is increased in CD_3OD (-6.9×10^{-4} ppm/K from 4.44ppm at -85°C, to 4.34ppm at 60°C). In DMSO however, there is no change in the chemical shift as the temperature is varied. No new information about the coupling constants could be obtained from this resonance, but at higher temperatures it does show the 1.3Hz coupling constant, proving that this is a ^5J coupling to the His α-proton.

Of the other resonances, at low temperatures (<-40°C), the phenyl resonances are resolved into *ortho*, *meta*, and *para* resonances. Between -40°C and 80°C, the *meta* and *para* resonances are merged, and at temperatures above 80°C, all the phenyl protons occur as a single multiplet. The amide resonances are not observed in CD_3OD, but in DMSO they gradually merge (complete at 110°C), and become less intense, almost disappearing at 130°C. As shown in Tables 1 and 2, the imidazole H2 resonance moves gradually to higher field as the temperature increases (-2.6×10^{-3} ppm/K in CD_3OD, and -3.4×10^{-3} ppm/K in DMSO). At higher temperatures, this peak also splits ito a doublet, presumably coupling to the imidazole H5 although the coupling is not observed in that resonance due to the peak being broader. The resonance due to the imidazole H5 also shows a shift to higher field as the temperature increases from -85°C to -30°C in CD_3OD (-1.6×10^{-3}

ppm/K), but at temperatures above -10°C this reverses and the resonance shifts downfield (in CD_3OD at a rate of 7.1×10^{-4} ppm/K, and in DMSO at a rate of 8.7×10^{-4} ppm/K).

By using the α–β coupling constants, it is possible to calculate the percentage populations of each conformer about the α–β bond from a Karplus equation[10]. It is normally assumed, that only the three possible staggered conformations are populated, and these are designated as t, g^+, and g^- as shown in Figure 3. In order to calculate the relative populations of these three states, two sets of parameters that are not readily available are required. The first of these is the coupling constant that would be observed between each H_α-H_β for each of the three conformations. Average values for these coupling constants were calculated from molecular modelling studies for the related diketopiperazine *cyclo*-[(S)-Trp-(S)-His][10], and used to derive the following three equations:-

$$^3J_{\alpha\beta} = 2.6g^+ + 2.4t + 12.1g^-$$

$$^3J_{\alpha\beta'} = 5.2g^+ + 12.4t + 2.7g^-$$

$$g^+ + t + g^- = 1$$

Figure 3: Newman Projections of the Three Staggered Conformers about a C_α-C_β Bond.

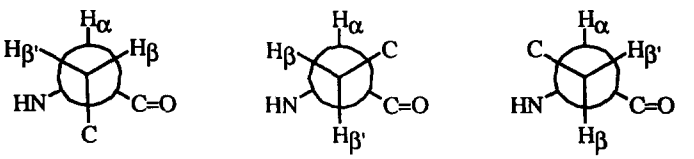

These equations have been used without modification to analyse the conformation of the unprotonated catalyst (1)[7], and are used again here. The second parameter needed before these equations can be used, is the diastereotopic assignment of the His and Phe β-protons (β and β' in Figure 3). In the case of catalyst (1), it has not been possible to unambiguously assign the diastereotopic His and Phe β-protons, so again use will be made of the theoretical predictions for *cyclo*-[(S)-Trp-(S)-His][10]. It was calculated that for the histidine residue, $^3J_{H\alpha H\beta'} > {}^3J_{H\alpha H\beta}$, so this was used to assign the higher field His-β proton as β'. In the case of the Phe residue, the calculations were carried out with both possible assignments and compared. The results of these calculations carried out over as wide a temperature range as possible are shown in Tables 3 and 4.

Table 3: Rotomer Populations about the His C_α-C_β Bond for Protonated Catalyst (1).

Temperature	Solvent	$g^\pm$	t	g^-
-40°C	CD_3OD	0.01	0.11	0.88
27°C	DMSO	0.27	0.12	0.61
60°C	CD_3OD	0.33	0.19	0.48
130°C	DMSO	0.40	0.13	0.47

Table 4: Rotomer Populations about the Phe C_α-C_β Bond for Protonated Catalyst (1).

Temperature	Solvent	Assignment	g^+	t	g^-
20°C	CD_3OD	high field=β'	0.90	-0.01	0.11
20°C	CD_3OD	low field=β'	0.90	0.11	-0.01
27°C	DMSO	high field=β'	0.87	0.01	0.12
27°C	DMSO	low field=β'	0.87	0.12	0.01
60°C	CD_3OD	high field=β'	0.80	0.00	0.20
60°C	CD_3OD	low field=β'	0.80	0.20	0.00
100°C	DMSO	high field=β'	0.71	0.05	0.24
100°C	DMSO	low field=β'	0.71	0.24	0.05

As can be seen from Table 3, the His residue spends most of its time in the g^- conformation, especially at low temperatures. As the temperature increases, the coupling constants indicate that the imidazole ring spends an increasingly significant amount of time folded over the diketopiperazine ring in the g^+ conformer, however there is no evidence of this in increased shielding of the phenyl CH_2 protons. Interestingly, the population of the t rotomer shows very little variation with temperature over a range of 170°C.

Examination of the results shown in Table 4, shows that the population of the g^+ conformer is independent of the assignment of the diastereotopic Phe-β protons (this is also true of the His residue). Thus at room temperature, the Phe residue is calculated to spend 90% of its time in the g^+ conformer, folded over the diketopiperazine ring, and shielding one of the His-β protons. As the temperature increases, the population of the g^+ rotomer decreases, and the His β-proton becomes less shielded. Depending upon the assignment of the diastereotopic protons, the results in Table 4 show that either the t or the g^- rotomer has a negligable population over the whole temperature range.

The above results are qualitively similar to those found in the same way for the unprotonated catalyst[7], although in that case the temperature range over which the populations were studied was much narrower. However the results in Tables 3 and 4 also show the limitation of this method in two ways. Firstly, one of the populations for the Phe-β protons is negative, indicating a slight error in one of the parameters. Secondly, it is well known that sterically only one residue can sit over the diketopiperazine (adopt the g^+ conformation) at any one time[10], however at 27°C the sum of the His and Phe g^+ conformations is 114%, again indicating an inaccuracy in the parameters. Thus although the results in Tables 3 and 4 appear to be qualitively correct, they are not quantitively accurate, and in particular the assignments to t and g^- could be reversed.

The same three conformer model can be used to explain the fact that the chemical shifts of the His β1, the Phe β2, and the Imidazole H5 protons first shift to higher field, then to lower field as the temperature is increased. The three conformations will have different energies, and hence different populations at any given temperature. For the His residue for example, the coupling constants suggest that the relative energies of the conformers will be $g^- < t < g^+$. Thus at low temperatures the observed chemical shifts will be those of the g^- rotomer as this will be the only one populated, and the chemical shift will not vary as the temperature is reduced further. As the temperature is increased however, the t rotomer will start to become significantly populated this will cause a change in the chemical shift (as it happens a shift to higher field). At still higher temperatures, the g^+ conformer will also start to become populated and exert an effect on the observed

chemical shift. This effect is seen as a shift back to low field. At a high enough temperature, all three rotomers will be approximately equally occupied, and the chemical shift should again be independent of temperature. The above argument has been given with the conformers having relative energies in the order $g^- < t < g^+$, but the same holds true whatever the order of the three conformers.

Molecular Modelling Results.

A molecular mechanics study of the protonated form of compound (1) was carried out using the Amber forcefield as implemented within the Macromodel program[11], running on a Silicon Graphics Personal Iris Workstation. A randomly drawn conformer of protonated (1), was first energy minimised using the TNCG method, to give a starting geometry. The entire conformational space available to the molecule was then searched *via* a grid search conducted at 60° resolution. All four freely rotatable bonds were rotated, as were the bonds within the diketopiperazine ring. Any conformer having unreasonable bond lengths within the diketopiperazine ring (less than 100 or greater than 200pm) was automatically discarded by the Macromodel program. The remaining conformers were energy minimised using the TNCG method, these calculations were carried out *in vacuo*, and in simulated chloroform and water solvents using the parameters within Macromodel. Inspection of the output at this stage revealed that the minimisation carried out in water had given a large number of conformers with similar energies and structures, so this set of conformers was further minimised using the FMNR method with line searching to give a final set unique conformers. The results from all three minimisations are shown in Tables 5-7, in each case all conformers within 10KJmol^{-1} of the global minimum energy conformation are recorded.

The results from the *in vacuo* calculations are clearly not compatable with the experimentally observed nmr results. A second conformer is predicted with a population of 37% which should be easily detected by nmr, but is not seen. The calculations in chloroform and water gave very similar results, in both cases conformers of type A are predicted to be the global minimum, and the ratio of the populations of type A/B is 8.0/1. It is worth noting, that all three sets of calculations predicted that conformations of type A would be the global minimum, this is in contrast to the results on the unprotonated compound where calculations carried out *in vacuo* predicted that type B would be the global minimum conformation[6]. Also the type A/B ratio has increased on protonating the imidazole ring, as the values calculated for the unprotonated compound were between 0.9 and 4.1 to 1.0, this is consistent with the experimentally observed results. The H_α-H_β coupling constants predicted by the Macromodel program (Tables 5-7) are also roughly consistent with those observed, especially at low temperature (Table 2).

As can be seen in Table 5, the results of the calculations carried out in water predict the presence of five type A conformations within 10KJmol^{-1} of the global minimum energy conformation (and one further type A conformation at -257.95KJmol^{-1}, not shown in Table 5). These conformers differ in the orientation of the imidazole ring which may adopt either the g^- or the t rotomer. In addition, three conformations of type C (with the imidazole ring in the g^+ rotomer) are also calculated to be of relatively low energy. This suggests, that as the temperature is raised these alternative conformers will become increasingly populated, and the imidazole ring will rotate about the α–β bond This is consistent with the variable temperature nmr results where the variation in the His CH_α-CH_β coupling constants suggest that as the temperature is raised, the imidazole ring rotates around the α–β bond. The results calculated in a chloroform solvent however, provide

no such indication of rotation about the His α–β bond, thus it appears that the calculations in water most accurately represent the structure of the protonated catalyst (1) in DMSO and methanol solvents.

Table 5: Molecular Mechanics Results on Protonated Compound 1. Calculated in Water.

Conformer Energy (KJ/Mol)	Population (%)[1]	Conformer Type[2]	Coupling Constants (H_α-H_β) (Hz)[3] His	Phe
-268.51	29.3	A (His g⁻)	11.8, 3.0	3.7, 2.9
-268.38	27.8	A (His t)	11.1, 1.6	4.0, 2.6
-266.78	14.6	A (His t)	11.8, 3.1	4.0, 2.6
-264.33	5.4	B	3.4, 3.0	4.4, 2.3
-263.70	4.2	B	3.4, 3.0	3.7, 2.9
-262.82	3.0	C (Phe t)	3.2, 3.2	11.8, 2.8
-262.76	2.9	D	3.6, 2.8	11.8, 3.1
-262.58	2.7	C (Phe g⁻)	3.2, 3.2	11.8, 2.9
-262.39	2.5	A (His g⁻)	11.1, 5.0	4.1, 2.6
-261.80	2.0	A (His t)	11.3, 4.8	4.8, 2.1
-261.02	1.4	D	11.4, 1.8	11.8, 3.2
-260.64	1.2	D	3.6, 2.8	11.8, 3.1
-260.34	1.1	D	11.4, 1.9	11.8, 3.1
-258.89	0.6	D	11.8, 3.1	11.8, 3.1

1) Populations are calculated at 298.15K. 2) Conformer type A has the phenyl ring folded over the diketopiperazine, type B has the two aromatic rings facing each other across the diketopiperazine, type C has the imidazole ring folded over the diketopiperazine, and type D is an assortment of other conformations. For an explanation of the t and g⁻ symbols, see text. 3) Coupling constants are calculated within the Macromodel program.

Table 6: Molecular Mechanics Results on Protonated Compound 1. Calculated in Chloroform

Conformer Energy (KJ/Mol)	Population (%)[1]	Conformer Type[2]	Coupling Constants (H_α-H_β) (Hz)[3] His	Phe
-137.19	81.1	A (His t)	11.1,1.6	3.9,2.7
-131.96	9.8	B	3.4,3.0	4.6,2.2
-129.43	3.5	D	3.5,3.0	11.8,3.3
-129.47	3.3	D	11.5,1.9	11.8,3.2
-127.76	1.8	B	3.4,3.0	4.6,2.2

Footnotes as for Table 5.

Table 7: Molecular Mechanics Results on Protonated Compound 1. Calculated in Vacuo.

Conformer Energy (KJ/Mol)	Population (%)[1]	Conformer Type[2]	Coupling Constants (H_α-H_β) (Hz)[3] His	Phe
3.55	62.8	A (His t)	11 3,1.7	3.8,2.7
4.85	37.2	B	3.5,2.9	4.4,2.3

Footnotes as for Table 5.

In one respect however, the molecular modelling results do not agree with the experimental data. All three sets of molecular mechanics calculations predict that the His residue will be predominately in the t rotomer, whilst the coupling constants suggest that the g^- rotomer will be occupied instead. The results calculated in water do show the g^- rotomer to be the global minimum, however the small energy difference between this and the other type A conformers with the His residue in the t rotomer indicates that except at very low temperatures, the t rotomer will be more highly populated as shown in Table 4. There are two possible explanations for this difference, firstly the molecular mechanics could be erroneously favouring the t rotomer by finding an intramolecular hydrogen bond between the 3'-NH of the imidazole and the histidine carbonyl. Secondly, the assignment of the diastereotopic His β–protons (which is based on theoretical calculations on a similar molecule[10]) could be incorrect. Thus would cause the populations of the t and g^- rotomers to be reversed. It is not clear at present which of these two factors is responsible for the inconsistency.

NMR Studies on the HCN Complex

Having established the expected spectrum for both unprotonated and protonated forms of (1), the nmr spectrum of a mixture of compound (1) and excess HCN was obtained and is shown in Figure 2c. It is immediately apparent, that this spectrum corresponds to the unprotonated form of the catalyst, and not to the protonated form. Two conformers are seen, and the Phe-β-CH_2 protons occur as a single resonance. That HCN was actually present in the solution was proven *via* a ^{13}C nmr spectrum which showed a very strong signal at 113.5ppm corresponding to HCN. (The same signal at 113.5ppm was observed in a sample composed of just HCN in DMSO-d_6) Hence it can be concluded, that the interaction between catalyst (1) and HCN is a covalent hydrogen bonded one, and that both conformations of compound (1) are present in the complex.

Conclusions

NMR studies suggest that upon protonation, catalyst (1) adopts a similar conformation to that of the major conformer of the unprotonated compound Variable temperature nmr studies indicate that rotation can occur about both the Phe and His α–β bonds, but that the Phe residue is largely present in the g^+ rotomer and the His residue in the g^- rotomer. These findings are largely supported by a molecular mechanics study provided water is used as the solvent for the calculations Addition of HCN to a DMSO solution of the catalyst (1) produces a spectrum which resembles the unprotonated rather than the protonated spectrum, thus it is concluded that the interaction between (1) and HCN is covalent rather than ionic.

Further mechanistic and synthetic studies on the catalyst (1) are currently underway and will be reported in due course.

Acknowledgements

The authors thank Peboc U.K. Ltd. for generous financial support, and Mr. E. Lewis for nmr work. D.J.P.H thanks the EEC social fund and Peboc U.K. Ltd. for a research studentship.

References

1) Jackson, W.R., Jacobs, H.A., Jayatilake, G.S., Matthews, B.R., Watson, K.G.; *Aust. J. Chem.*, **1990**, 43, 2043; Becker, W., Freund, H., Pfeil, E., *Angew. Chem., Int. Ed. Engl.*, **1965**, 4, 1079; Brussee, J., Roos, E.C., v.d.Gen, A.; *Tetrahedron Lett.*, **1988**, 29, 4485; Ziegler, T., Horsch, B., Effenberger, F.; *Synthesis*, **1990**, 575; Matthews, B.R., Gountzos, H., Jackson, W.R., Watson, K.G.; *Tetrahedron Lett.*, **1989**, 30, 5157; Jackson, W.R., Jacobs, H.A., Matthews, B.R., Jayatilake, G.S., Watson, K.G.; *Tetrahedron Lett.*,**1990**, 31, 1447.

2) March, J., 'Advanced Organic Chemistry: Reactions, Mechanisms, and Structure 2nd Ed.', McGraw Hill, London, 1977, p873

3) Becker, W., Pfeil, E.; *J. Am. Chem. Soc.*, **1966**, 88, 4299; Becker, W., Freund, H., Pfeil, E.; *Angew. Chemie., Int. Ed. Engl.*, **1965**, 4, 1079; Ziegler, T., Horsch, B., Effenberger, F.; *Synthesis*, **1990**, 575; Effenberger, F., Horsch, B., Weingart, F., Ziegler, T., Kuhner, S., *Tetrahedron Letts.*, **1991**, 32, 2605; Zandbergen, P., v.d.Linden, J., Brussee, J., v.d.Gen, A.; *Syn. Commun.*, **1991**, 21, 1387; Wilms, E.S., Brussee, J., v.d.Gen, A., v.Scharrenburg, G.J.M., Sloothaak, J.B.; *Recuil des Travaux Chimiques des Pays-Bas*, **1991**, 110, 209; Ognyanov, V.I., Datcheva, V.K., Kyler, K.S.; *J. Am. Chem. Soc.*, **1991**, 113, 6992; Reetz, M.T., Kunisch, F., Heitmann, P.; *Tetrahedron Letts.*, **1986**, 27, 4721; Narasaka, K., Yamada, T., Minamikawa, H.; *Chem. Letts.*, **1987**, 2073; Minamikawa, H., Hayakawa, S., Yamada, T., Iwasawa, N., Narasaka, K.; *Bull. Chem. Soc. Jpn.*, **1988**, 61, 4379; Hayashi, M., Matsuda, T., Oguni, N.; *J. Chem. Soc., Chem. Commun.*, **1990**, 1364; Mori, A., Ohno, H., Nitta, H., Tanaka, K., Inoue, S.; *Synlett.*, **1991**, 563; Mori, A., Nitta, H., Kudo, M., Inoue, S., *Tetrahedron Letts.*, **1991**, 32, 4333; Kobayashi, S., Tsuchiya, Y., Mukaiyama, T., *Chem. Letts.*, **1991**, 541; Danda, H., Chino, K., Wake, S.; *Chem. Letts.*, **1991**, 731; Gountzos, H., Jackson, W.R., Harrington, K.J.; *Aust. J. Chem.*, **1986**, 39, 1135; Danda, H.; *Bull. Chem. Soc. Jpn.*, **1991**, 64, 3743.

4) Oku, J., Inoue, S.; *J. Chem. Soc., Chem. Commun.*, **1981**, 229; Oku, J., Ito, N., Inoue, S.; *Makromol. Chem.*, **1982**, 183, 579; Asada, S., Kobayashi, Y., Inoue, S., *Makromol. Chem.*, **1985**, 186, 1755; Kobayashi, Y., Asada, S., Watanabe, I., Hayashi, H., Motoo, Y., Inoue, S.; *Bull. Chem. Soc. Jpn.*, **1986**, 59, 893; Jackson, W.R., Jayatilake, G.S., Matthews, B.R., Wilshire, C.; *Aust. J. Chem.*, **1988**, 41, 203; Matthews, B.R., Jackson, W.R., Jayatilake, G.S., Wilshire, C., Jacobs, H.A.; *Aust. J. Chem.*, **1988**, 41, 1697; Tanaka, K., Mori, A., Inoue, S.; *J. Org. Chem.*, **1990**, 55, 181; Danda, H., Nishikawa, H., Otaka, K.; *J. Org. Chem.*, **1991**, 56, 6740; Danda, H.; *Synlett.*, **1991**, 263.

5) Oku, J., Ito, N., Inoue, S.; *Makromol Chem.*, **1979**, 180, 1089; Mori, A., Ikeda, Y., Kinoshita, K., Inoue, S.; *Chem. Lett.*, **1989**, 2119.

6) North, M.; *Tetrahedron*, **1992**, 48, 5509.

7) Callant, D., Coussens, B., v.d.Maten, T., de Vries, J., de Vries, N.K.; *Tetrahedron Asymmetry*, **1992**, 3, 401.

8) Deslauriers, R., Grzonka, Z., Schaumburg, K., Shiba, T., Walter, R.; *J. Am. Chem. Soc.*, **1975**, 97, 5093.

9) Davies, D.B., Khaled, Md.A.; *J. Chem. Soc , Perkin Trans. II*, **1976**, 1238.

10) Sheinblatt, M., Andorn M., Rudi, A.; *Int. J. Pept. Prot Res* , **1988**, 31, 373.

11) Still, W.C., Mohmadi, F., Richards, N.G.J., Guida, W.C., Lipton, M., Liskamp, R., Chang, G., Hendrickson, T., DeGunst, F., Hasel, W.; Macromodel 3D., Version 3.1, Columbia Univesrsity, New York, NY, 1991.